

# Cell-of-origin of diffuse large B-cell lymphomas determined by the Lymph2Cx assay: better prognostic indicator than Hans algorithm

Nara Yoon<sup>1</sup>, Soomin Ahn<sup>2</sup>, Hae Yong Yoo<sup>3</sup>, Suk Jin Kim<sup>4</sup>, Won Seog Kim<sup>4</sup>, Young Hye Ko<sup>5</sup>

<sup>1</sup>Department of Pathology, The Catholic University of Korea Incheon St. Mary's Hospital, Incheon, Korea

<sup>2</sup>Department of Pathology, Ewha Womans University Medical Center, Ewha Womans University School of Medicine, Seoul, Korea

<sup>3</sup>Department of Health Sciences and Technology, Samsung Advanced Institute for Health Sciences and Technology, Sungkyunkwan University, Seoul, Korea

<sup>4</sup>Division of Hematology and Oncology, Department of Medicine, Samsung Medical Center, Sungkyunkwan University School of Medicine, Seoul, Korea

<sup>5</sup>Department of Pathology and Translational Genomics, Samsung Medical Center, Sungkyunkwan University School of Medicine, Seoul, Korea

**Correspondence to:** Young Hye Ko, **email:** yhko310@skku.edu

**Keywords:** lymphoma, large B-cell, diffuse, gene expression profiling, Lymph2Cx

**Received:** January 09, 2017

**Accepted:** January 29, 2017

**Published:** February 28, 2017

## ABSTRACT

**Diffuse large B-cell lymphomas (DLBCLs) are clinically heterogeneous and need a biomarker that can predict the outcome of treatments accurately. To assess the prognostic significance of the cell-of-origin type for DLBCLs, we applied the Lymph2Cx assay using a NanoString gene expression platform on formalin-fixed paraffin wax-embedded pretreatment tissues obtained from 82 patients with *de novo* DLBCL, not otherwise specified. All patients were treated with rituximab plus cyclophosphamide, doxorubicin, vincristine, and prednisone (R-CHOP) as the first line of chemotherapy. Based on the expression levels of Bcl-6, CD10, and MUM-1 measured by immunohistochemistry, cases were subdivided into germinal center B-cell (GCB) and non-GCB types according to the Hans algorithm. NanoString assay was performed on 82 cases. The Lymph2Cx assay successfully classified 82 cases into three categories: activated B-cell (ABC), GCB, and unclassified types. The concordance rate between the Lymph2Cx assay and the Hans algorithm was 73.6%. The Lymph2Cx-defined ABC type had significantly poorer outcomes compared with the GCB type (5-year overall survival, GCB vs. ABC, 96.6% vs. 77.1%,  $P = 0.020$ ; 5-year disease-free survival, GCB vs. ABC, 96.6% vs. 79.2%,  $P = 0.018$ ). In contrast, no significant differences were observed in survival between the two patient subgroups with DLBCL types classified by the Hans algorithm. The Lymph2Cx assay is a robust, reliable method for predicting the outcome of patients with DLBCL treated with R-CHOP chemotherapy.**

## INTRODUCTION

Diffuse large B-cell lymphoma (DLBCL) is the most frequent type of non-Hodgkin's malignant lymphoma comprising 30–40% of adult lymphomas [1] and is a clinically heterogeneous disease showing unpredictable outcomes [2–5]. The most powerful prognostic factor is

the International Prognostic Index (IPI) based on clinical and biochemical parameters including age, Eastern Cooperative Oncology Group (ECOG) performance status, tumor stage, extranodal involvement, and lactate dehydrogenase (LDH) level [4, 6]. In 2000, Alizadeh *et al.* used “Lymphochip” cDNA microarrays and found that the “Cell-of-Origin” (COO) of DLBCL could be divided

into activated B-cell (ABC) and germinal center B-cell (GCB) types, with significant prognostic values [7]. The Leukemia Lymphoma Molecular Profiling Project applied the same microarray gene expression profiling (GEP) to an expanded cohort and identified three subgroups within DLBCL: ABC, GCB, and unclassified subgroups. This suggested that a GEP-defined COO might serve as an independent prognostic biomarker [8]. The GCB subtype appears to arise from germinal-center B cells and is associated with two molecular events: recurrent gene (14:18) translocations involving *BCL-2* and *C-REL* amplification [2, 8–10]. The ABC subtype might arise from a post-germinal center B cell and has frequent amplifications of the oncogene *SPIB*, recurrent trisomy for chromosome 3, and activation of the antiapoptotic nuclear factor (NF)- $\kappa$ B signaling pathway [2, 8–11].

The microarray-based GEP technique using RNA extracted from frozen tissue was the original standard for determining the COO type of DLBCL [10, 12]. With limited access to frozen samples, immunohistochemistry (IHC)-based classifications have been developed during the past decade [13–16]. Among them, the Hans algorithm, a classification based on three antibodies (CD10, BCL6, and MUM1) is widely used in place of microarrays [12, 15]. However, its inherent subjectivity and variability in scoring, lowers the reliability of such IHC-based methodology [17–21].

The nCounter platform of NanoString Technologies (Seattle, WA, USA) is useful for the direct multiplex measurement of gene expression using formalin-fixed paraffin wax-embedded (FFPE) tissues, and various clinical research studies using this platform have been performed [22–30]. Scott *et al.* [31] have recently published a 20-gene version of a NanoString code set for a COO typing assay of DLBCL named Lymph2Cx. Fifteen genes, along with five housekeeping genes, were selected among 93 genes, which were identified based on their ability to accurately replicate the COO model of Lenz *et al.* [9, 31] Here, we applied the Lymph2Cx NanoString nCounter gene expression system to FFPE pretreatment tissue samples from 82 patients with DLBCL and evaluated its predictive value compared with the Hans algorithm.

## RESULTS

### Patient population

The study included 51 (62.2%) male and 31 (37.8%) female patients, with a mean age of 60 years (range 18–82). Of these, 73 (89%) patients had a good performance status (ECOG grade 0 or 1). More than two-thirds (70.7%) had extranodal lymphomas and the rest (29.3%) had nodal lymphomas (Table 1). The extranodal sites included in our study are the following: stomach, colon, small intestine, appendix, breast, spleen, testis, brain, head and neck,

thyroid, kidney, soft tissue, ovary, bone, and heart. As for the distribution of IPI populations, forty nine (59.8%) cases were categorized as low IPI risk group (0-1), 15 (18.3%) cases as low Intermediate (2), 10 (12.2%) cases as high intermediate (3), 8 (9.8%) cases as high score (4-5). Follow-up data were available for all cases with a mean follow-up of 50 months (range 0–145).

### COO assay by Lymph2Cx

This cohort consisted of 43 non-GCB and 39 GCB DLBCLs, as classified by the Hans algorithm. All FFPE samples yielded sufficient RNA for the NanoString technology analyses. The results of the COO assay by Lymph2Cx are summarized in Table 2. Of the 82 cases, 48 (58.5%) were classified as ABC; 29 (35.4%) as GCB, and five (6.1%) were unclassified by Lymph2Cx. Of 43 non-GCB cases classified by the Hans algorithm, 36 (83.7%) were classified as ABC, three (7.0%) as GCB, and four (9.3%) were unclassified by the Lymph2Cx assay. In 39 GCB cases classified by the Hans algorithm, 12 (30.8%) were classified as ABC, 26 (66.7%) as GCB, and one (2.6%) was unclassified by the Lymph2Cx assay. The overall concordance rate between the COO determined by the Hans algorithm and the Lymph2Cx assay was 73.6%, 80.5% when unclassified cases were removed

### Clinical characteristics of COO groups classified by the Lymph2Cx assay or the Hans algorithm

Clinical correlations with COO subgroups classified by the Lymph2Cx assay or the Hans algorithm are shown in Table 1. Compared with the GCB type, patients were significantly older in those classified as having a non-GCB type by the Hans algorithm ( $P = 0.002$ ), and having an ABC type or unclassified by the Lymph2Cx subtype ( $P = 0.016$ ). Gender, primary sites, ECOG performance scores, serum LDH levels, Ann Arbor tumor stage, extranodal site number, and IPI showed no associations.

### Univariate survival analysis

Kaplan–Meier plots of OS and DFS showed distinct differences in the 5-year patient survival rates between COO types classified using the Lymph2Cx system. Those with the GCB type had an improved 5-year OS (GCB vs. ABC vs. unclassified: 96.6% vs. 77.1% vs. 60%, respectively;  $P = 0.026$ ) and 5-year DFS (GCB vs. ABC vs. unclassified: 96.6% vs. 79.2% vs. 60%, respectively;  $P = 0.021$ ) compared with the ABC and unclassified types categorized by the Lymph2Cx method (Figure 1). Patients with the unclassified type of tumor had the worst OS and DFS rates. Patients with the COO type determined by the Hans algorithm showed no significant differences in 5-year OS ( $P = 0.749$ ) or 5-year DFS rates ( $P = 0.155$ ) between the GCB and non-GCB groups (Figure 1).

**Table 1: Associations between clinical features and COO types determined by the Hans algorithm and Lymph2Cx assay**

Characteristics	Total (n = 82)	COO assay by Hans algorithm, n (%)			COO assay by Lymph2Cx, n (%)			
		GCB (n = 39)	Non-GCB (n = 43)	P	GCB (n = 29)	ABC (n = 48)	Unclassified (n = 5)	P
Gender:				0.734				0.977
Male	51 (62.2)	25 (64.1)	26 (60.5)		19 (65.5)	28 (58.3)	4 (80.0)	
Female	31 (37.8)	14 (35.9)	17 (39.5)		10 (34.5)	20 (41.7)	1 (20.0)	
Primary site:				0.776				0.682
Nodal	24 (29.3)	12 (30.8)	12 (27.9)		8 (27.6)	16 (33.3)	0 (0)	
Extranodal	58 (70.7)	27 (69.2)	31 (72.1)		21 (72.4)	32 (66.7)	5 (100)	
Age, years:				0.002*				0.016*
≤ 60	40 (48.8)	26 (66.7)	14 (32.6)		20 (69.0)	18 (37.5)	2 (40.0)	
> 60	42 (51.2)	13 (33.3)	29 (67.4)		9 (31.0)	30 (62.5)	3 (60.0)	
ECOG performance status:				0.613				0.823
< 2	73 (89.0)	34 (87.2)	39 (90.7)		26 (89.7)	42 (87.5)	5 (100)	
≥ 2	9 (11.0)	5 (12.8)	4 (9.3)		3 (10.3)	6 (12.5)	0 (0)	
Serum LDH:				0.882				0.647
Normal	54 (65.9)	26 (66.7)	28 (65.1)		21 (72.4)	30 (62.5)	3 (60.0)	
Elevated	28 (34.1)	13 (33.3)	15 (34.9)		8 (27.6)	18 (37.5)	2 (40.0)	
Stage:				0.750				0.630
< 3	54 (65.9)	25 (64.1)	29 (63.4)		21 (72.4)	29 (60.4)	4 (80.0)	
≥ 3	28 (34.1)	14 (35.9)	14 (32.6)		8 (27.6)	19 (39.6)	1 (20.0)	
Extranodal involvement:				0.841				0.286
< 2	68 (82.9)	32 (82.1)	36 (83.7)		26 (89.7)	38 (79.2)	4 (80.0)	
≥ 2	14 (17.1)	7 (17.9)	7 (16.3)		3 (10.3)	10 (20.8)	1 (20.0)	
IPI grade:				0.869				0.566
Low (0–1)	49 (59.8)	22 (56.4)	27 (62.8)		18 (62.1)	27 (56.3)	4 (80.0)	
Intermediate (2–3)	25 (30.5)	14 (35.9)	11 (25.6)		10 (34.5)	15 (31.3)	0 (0)	
High (4-5)	8 (9.8)	3 (7.7)	5 (11.6)		1 (3.4)	6 (12.5)	1 (20.0)	

COO, cell of origin; ABC, activated B-like cell; GCB, germinal center B-like; ECOG, Eastern Cooperative Oncology Group performance; LDH, lactate dehydrogenase; IPI, international prognostic index.

When the unclassified groups were excluded from the Lymph2Cx data, the differences in 5-year OS (GCB vs. ABC, 96.6% vs. 77.1%;  $P = 0.020$ ) (Supplementary Figure 1) and 5-year DFS (GCB vs. ABC, 96.6% vs. 79.2%;  $P = 0.018$ ) (Supplementary Figure 2) remained significant.

### Multivariate survival analysis

IPI scores 0–1 vs. 2–5 and the COO type determined by the Lymph2Cx assay were combined in a multivariate Cox Proportional Hazards model; this revealed that both were independent predictors of 5-year OS and DFS rates (Table 3).

**Table 2: Comparison between the Hans algorithm and Lymph2Cx assay**

		COO by Lymph2Cx, n (%)			
		ABC (n = 48)	GCB (n = 29)	Unclassified (n = 5)	P
COO by Hans algorithm; n (%)	Non-GCB (n = 43)	36 (75.0)	3 (10.3)	4 (80.0)	< 0.001
	GCB (n = 39)	12 (25.0)	26 (89.7)	1 (20.0)	

COO, cell of origin; ABC, activated B-like cell; GCB, germinal center B-like.

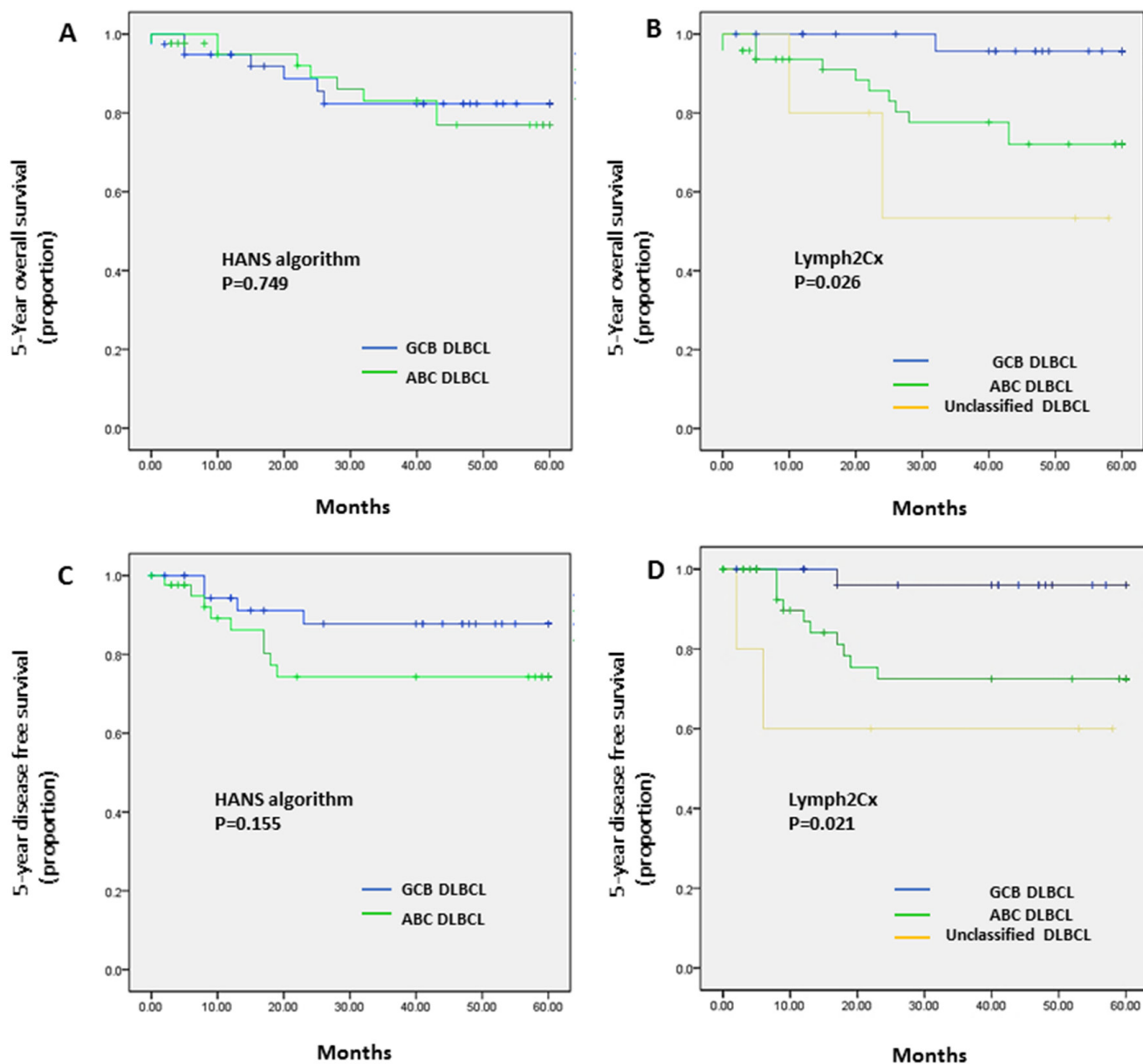


**Figure 1: Kaplan–Meier analysis of 5-year OS and DFS in the patients with DLBCL types classified by the Hans algorithm A., C. or the Lymph2Cx assay B., D.** (A) COO assay by the Hans algorithm showed no difference in 5-year OS ( $P = 0.749$ ) between GCB and non-GCB types. (B) Lymph2Cx-defined GCB type gave the most favorable outcome among three Lymph2Cx-defined subgroups (GCB vs. ABC vs. unclassified; 96.6% vs. 77.1% vs. 60%, respectively;  $P = 0.026$ ). (C) COO assay by the Hans algorithm showed no difference in the 5-year DFS rate ( $P = 0.155$ ) between the GCB and non-GCB types. (D) The Lymph2Cx-defined GCB type had the best patient survival among the three subgroups (GCB vs. ABC vs. unclassified; 96.6% vs. 79.2% vs. 60%, respectively;  $P = 0.021$ ).

**Table 3: Multivariate survival analyses with combined IPI scores (0–1 vs. 2–5) and the COO determined by the Lymph2Cx assay**

Variable	Unfavorable category	5-year OS			5-year DFS		
		HR	95% CI	P	HR	95% CI	P
COO by Lymph2Cx				0.024*			0.029*
	ABC	7.840	1.011–60.784	0.049	7.654	0.979–59.873	0.052
	Unclassified	33.669	2.700–419.908	0.006	30.449	2.454–377.770	0.008
IPI score	Intermediate/High	5.119	1.423–18.417	0.012*	3.518	1.010–12.253	0.048*

COO, Cell of origin; IPI, international prognostic index; OS, overall survival; DFS, disease free survival; HR, hazard ratio; CI, confidence interval.

## DISCUSSION

The development of DNA microarray techniques has provided effective tools for exploring the molecular features of DLBCL and has provided knowledge of specific genes associated with particular responses to chemotherapy [7, 8, 10, 31–34]. Although microarray GEP approaches are standard methods for determining the COO type of DLBCL [7, 8, 10], they are expensive and have poor flexibility and reproducibility when evaluating low-quality RNA samples, especially from FFPE samples; moreover, they still require RNA extraction from frozen tissues for high quality data [22, 24–26, 32]. For this reason, despite its high accuracy, microarray-based COO profiling is not applicable in clinical practices in which FFPE samples are used widely.

IHC-based methodology is rapid, cost-effective and readily available, so it has been widely developed and adopted in clinical practice and research [14–16, 33]. The Hans algorithm subdivides cases into GCB or non-GCB types by combining the results for the CD10, BCL-6, and MUM1 antibodies [15]. This algorithm showed 80% concordance with the GEP classification and similar patient survival outcomes [15]. The Choi algorithm adding FOXP1 and GCET1 to Hans algorithm also demonstrated high concordance (93%) with a GEP classification [12]. A Tally method substituting BCL6 for the LMO2 antibody showed a better ability to predict COO than other IHC-based algorithms [16]. The three algorithms were recently compared with GEP in 108 biopsy samples, and the study showed that the Hans and Choi algorithms were significantly more predictive of OS and progression-free survival (PFS) than the Tally method [34]. However, the value of IHC methods for assessing COO has become questionable because of poor concordance with GEP methods, inferior accuracy and reproducibility, and a lack of prognostic utility [4, 11, 15–19]. Accordingly, there is a need for developing reproducible, reliable and clinically applicable techniques for assessing the COO types in patients with DLBCL.

The NanoString technology uses digitally colored code sets that are attached to sequence-specific probes. By direct measurement of mRNA, it offers highly sensitive, reproducible and fully quantitative results on FFPE and frozen tissue samples [22, 23, 32, 35–37]. The technique covers a large number of genes, enables complex genomic analysis including the detection of gene fusions, and requires a low RNA input of as little as 200 ng. A previous study demonstrated a strong concordance between patient-matched frozen and FFPE material, showing the applicability of the NanoString platform to FFPE samples [22]. Scott *et al.* [31] selected 20 of the most predictive genes of a NanoString code set for the COO assay and generated a predictive model named Lymph2Cx, and the scores produced by two independent laboratories showed a very high concordance.

In this study, we applied the Lymph2Cx assay to 82 FFPE pretreatment samples from patients with DLBCLs who were treated with R-CHOP and compared it with the Hans algorithm. The correlation between the Hans algorithm and the Lymph2Cx assay was poor, with a discordancy rate of 26.4%. Of cases classified as ABC by the Lymph2Cx assay, 25% were misclassified as GCB by the Hans algorithm and 3% of cases classified as GCB by the lymph2Cx assay were misclassified as non-GCB by the Hans algorithm. We re-reviewed IHC slides of 12 GCB cases by Hans reclassified as ABC by Lymph2Cx. Eleven of 12 cases showed diffuse positivity for CD10 in more than 75% of tumor cells without background overstaining. One case with CD10 negativity was diffusely positive for BCL6 and negative for MUM1. Regarding BCL-6, 12 cases were positive with more than 60%. MUM1 was also diffusely positive for 11 cases without background stain. Therefore, misclassification based on the Hans algorithm does not seem to be caused by technical error of IHC.

The Hans algorithm has been reported to have a misclassification rate of 19.7% when compared with GEP data; this might arise from technical factors related to staining, interpretation, and scoring of the data [18, 38]. However, Barrans *et al.* pointed out that decision trees of IHC algorithms use sequential rather than parallel

**Table 4: Immunohistochemical and clinical findings of unclassified DLBCL types determined by the Lymph2Cx assay**

Case No.	CD10 (%)	BCL6 (%)	MUM1 (%)	Han's algorithm	Recurrence	Death from DLBCL progression	Clinicopathological history
1	0	5	95	ABC	Yes	Yes	Reactivated TB
2	0	30	70	ABC	No	No	
3	0	40	70	ABC	Yes	Yes	Synchronous EGC (submucosal); HBV carrier
4	0	90	40	ABC	No	No	C-MYC FISH+
5	90	95	70	GCB	No	No	

TB, tuberculosis; EGC, early gastric cancer; HBV, hepatitis B virus.

consideration of markers, inherently fail to capture the overall pattern of gene expression, and lead to a lack of clinical correlation [17].

It is well established that patients with the GCB type of COO show significantly better OS than those with the ABC type by GEP classification [7, 8, 20, 33, 39]. Our COO typing assay made using the Lymph2Cx system, maintained the same prognostic significance as previous reports [9, 31, 35]. The Lymph2Cx-defined ABC type patient groups had significantly worse outcome than those with the GCB type whereas the COO types assigned by the Hans algorithm did not show significantly different outcomes in this cohort.

Distinct from the binary IHC groups, a third type of COO has been recognized in GEP studies in which the tumor cannot be assigned to either GCB or ABC groups [8]. This biologically distinct subgroup was named “type 3” and is now known as “unclassified” [8, 40]. In this study, five (6.1 %) cases labeled as the unclassified type had the worst outcome among all three groups as determined by the Lymph2Cx assay. This was inconsistent with previous Lymph2Cx results, in which the unclassified group of patients was shown to have an intermediate prognosis between the GCB and ABC types [31, 35]. Of five unclassified DLBCLs, two patients had recurrence and died of tumor progression. The poor survival for this type might have an association with underlying infectious diseases that compromised the patient’s condition leading to cancer progression. One patient (#1) had a history of tuberculosis (TB) and this had been reactivated at the time of death. The second patient (#3) was a carrier of the Hepatitis B virus (HBV) and had synchronous early gastric cancer (Table 4). The study of Barrans *et al.* [17] presented the best survival of patients with unclassified DLBCLs (designated as Type III in their study), but this differed from a previous GEP study [8]. They speculated that this disagreement arose from the different mix of cases in their cohort showing that a number of different entities were likely to be included in the Type III group, including DLBCL of T-cell rich type and DLBCL

presenting in extranodal sites [17]. Their data along with ours suggest that unclassified types of DLBCL might have variable clinical outcomes because of the heterogeneity of study populations. This phenomenon was emphasized by a relatively smaller proportion of the unclassified group, comprising about 5–15% of DLBCLs [31, 40].

The limitation of our study is that the patient population is not representative of typical nodal DLBCL. We selected mainly surgical specimens rather than biopsy tissues for evaluation of whole protein expression pattern by immunohistochemistry. Therefore, extranodal sites were overly selected. In addition, there are some differences in patient population between ours and previous studies [31, 35]. Compared to Scott *et al.*'s series, this study had more low-stage disease, more low-IPI score, a lower proportion of GCB cases, and better OS rates [31, 35]

## Conclusion

In this study, the Lymph2Cx assay could divide DLBCLs into three molecular subgroups with distinctive prognoses, whereas the IHC-based Hans algorithm failed to reproduce this. Thus, the Lymph2Cx assay could predict survival independent of the IPI score and was successfully applied to FFPE tissue samples.

## MATERIALS AND METHODS

We retrospectively evaluated pretreatment samples taken from 100 patients with DLBCL who underwent excisional biopsy including resection of solid organs before chemotherapy in Samsung Medical Center between 2004 and 2015. Representative FFPE tissues of the 100 cases were selected from the archived histopathology files of Samsung Medical Center. A hematoxylin and eosin-stained section from each sample was assessed to confirm the diagnoses and tumor content. After experiments, patients who were not treated with rituximab plus cyclophosphamide,

doxorubicin, vincristine, and prednisone (R-CHOP) or those with post-transplant lymphoproliferative and Epstein–Barr virus (EBV)-positive DLBCL tumors were excluded, as well as one patient who died of diabetic renal disease, by reviewing electronic medical records. Finally, 82 cases of DLBCL, not otherwise specified (NOS) remained for data analysis.

### Ethics statement

The study was approved by the institutional review board of the Samsung Medical Center (IRB NO:2011-11-056).

### CD10, BCL-6, and MUM-1 detection with IHC

IHC was performed for CD10, BCL6, and MUM1 antibodies at the time of the initial diagnosis. FFPE tissues were cut into 4  $\mu$ m sections and then stained using an automated system (Technomate 1000, DakoCytomation, DAKO, Glostrup, Denmark) using a standard method. The samples were analyzed semi-quantitatively by two pathologists (N. Yoon and Y. Ko). Based on the Hans algorithm, CD10, BCL6, and MUM1 expression levels were evaluated with 30% cutoff values for the proportions of tumor cells stained. Consensus on discordant cases was reached by a joint review on a multi-head microscope.

### NanoString-based multigene assay

NanoString assay was performed according to literature published [31]. The probe sequences, the procedures, an aliquot of the oligonucleotide standards were kindly provided by Prof. Rimsza L. at Mayo clinic. Total RNA was extracted from two 4- $\mu$ m thick sections from FFPE tumor tissues using High Pure RNA Paraffin kits (Roche Diagnostic, Mannheim, Germany) after removing non-tumorous elements by manual macrodissection guided by consulting the hematoxylin and eosin-stained slides. Nucleic acids were extracted using Qiagen AllPrep FFPE kits (Qiagen, Hilden, Germany), and digital GEP was performed on 200 ng aliquots of RNA using NanoString technology. The Lympho2Cx code set (Nanostring Technologies, Seattle, WA, USA) was used for gene expression analyses. The data were normalized to the mean expression levels of internal reference genes with cut off value 20. Standard QC was employed by nSolver™ Analysis Software (NanoString Technologies, WA) with flagging of any sample with a total of the positive spike-in controls being outside of 0.3 to 3 times the geometric mean of the total positive spike-in for that cartridge [31]. Data processing and the determination of COO type were done through the website <https://llmpp.nih.gov/LYMPHCX/index.shtml>.

### Statistical analysis

Statistical analysis was performed using SPSS statistical software (v. 20.0; IBM Corp., Armonk, NY, USA). Clinicopathological associations with COO types derived by the Lymph2Cx assay and the Hans algorithm were analyzed using chi-squared tests and linear-by-linear association. Overall survival (OS) and disease-free survival (DFS) rates of the patients with particular COO types were estimated using Kaplan–Meier and multivariate Cox Proportional Hazards analyses. A *p*-value < 0.05 was considered significant.

### ACKNOWLEDGMENTS

We thank Drs Lisa Rimsza and David W. Scott who generously provided gene sequences and links to the website for analysis.

### CONFLICTS OF INTEREST

The authors declare no conflicts of interest.

### FUNDING

This study was supported by a grant by the National Research Foundation of Korea (NRF-2014R1A2A2A01007826), and a grant of the Korea Health Technology R&D Project through the Korea Health Industry Development Institute (KHIDI) funded by the Ministry of Health & Welfare, Republic of Korea (HI14C3414).

### REFERENCES

1. Swerdlow SH, Campo E, Harris NL, Jaffe ES, Pileri SA, Stein H, Thiele J, Vardiman JW. WHO Classification of Tumours of Haematopoietic and Lymphoid Tissues. 4th ed. Lyon, France: IARC Press; 2008.
2. Bea S, Zettl A, Wright G, Salaverria I, Jehn P, Moreno V, Burek C, Ott G, Puig X, Yang L, Lopez-Guillermo A, Chan WC, Greiner TC, et al. Diffuse large B-cell lymphoma subgroups have distinct genetic profiles that influence tumor biology and improve gene-expression-based survival prediction. *Blood*. 2005; 106:3183-3190.
3. Coiffier B, Lepage E, Briere J, Herbrecht R, Tilly H, Bouabdallah R, Morel P, Van Den Neste E, Salles G, Gaulard P, Reyes F, Lederlin P, Gisselbrecht C. CHOP chemotherapy plus rituximab compared with CHOP alone in elderly patients with diffuse large-B-cell lymphoma. *N Engl J Med*. 2002; 346:235-242.
4. Nyman H, Adde M, Karjalainen-Lindsberg ML, Taskinen M, Berglund M, Amini RM, Blomqvist C, Enblad G, Leppa S. Prognostic impact of immunohistochemically defined germinal center phenotype in diffuse large B-cell lymphoma

- patients treated with immunochemotherapy. *Blood*. 2007; 109:4930-4935.
5. Sehn LH, Donaldson J, Chhanabhai M, Fitzgerald C, Gill K, Klasa R, MacPherson N, O'Reilly S, Spinelli JJ, Sutherland J, Wilson KS, Gascoyne RD, Connors JM. Introduction of combined CHOP plus rituximab therapy dramatically improved outcome of diffuse large B-cell lymphoma in British Columbia. *J Clin Oncol*. 2005; 23:5027-5033.
  6. Ziepert M, Hasenclever D, Kuhnt E, Glass B, Schmitz N, Pfreundschuh M, Loeffler M. Standard International prognostic index remains a valid predictor of outcome for patients with aggressive CD20+ B-cell lymphoma in the rituximab era. *J Clin Oncol*. 2010; 28:2373-2380.
  7. Alizadeh AA, Eisen MB, Davis RE, Ma C, Lossos IS, Rosenwald A, Boldrick JC, Sabet H, Tran T, Yu X, Powell JI, Yang L, Marti GE, et al. Distinct types of diffuse large B-cell lymphoma identified by gene expression profiling. *Nature*. 2000; 403:503-511.
  8. Rosenwald A, Wright G, Chan WC, Connors JM, Campo E, Fisher RI, Gascoyne RD, Muller-Hermelink HK, Smeland EB, Giltman JM, Hurt EM, Zhao H, Averett L, et al. The use of molecular profiling to predict survival after chemotherapy for diffuse large-B-cell lymphoma. *N Engl J Med*. 2002; 346:1937-1947.
  9. Lenz G, Wright G, Dave SS, Xiao W, Powell J, Zhao H, Xu W, Tan B, Goldschmidt N, Iqbal J, Vose J, Bast M, Fu K, et al. Stromal gene signatures in large-B-cell lymphomas. *N Engl J Med*. 2008; 359:2313-2323.
  10. Barton S, Hawkes EA, Wotherspoon A, Cunningham D. Are we ready to stratify treatment for diffuse large B-cell lymphoma using molecular hallmarks? *Oncologist*. 2012; 17:1562-1573.
  11. Dunleavy K, Pittaluga S, Czuczman MS, Dave SS, Wright G, Grant N, Shovlin M, Jaffe ES, Janik JE, Staudt LM, Wilson WH. Differential efficacy of bortezomib plus chemotherapy within molecular subtypes of diffuse large B-cell lymphoma. *Blood*. 2009; 113:6069-6076.
  12. Rimsza LM, Wright G, Schwartz M, Chan WC, Jaffe ES, Gascoyne RD, Campo E, Rosenwald A, Ott G, Cook JR, Tubbs RR, Braziel RM, Delabie J, et al. Accurate classification of diffuse large B-cell lymphoma into germinal center and activated B-cell subtypes using a nuclease protection assay on formalin-fixed, paraffin-embedded tissues. *Clin Cancer Res*. 2011; 17:3727-3732.
  13. Coutinho R, Clear AJ, Owen A, Wilson A, Matthews J, Lee A, Alvarez R, Gomes da Silva M, Cabecadas J, Calaminici M, Gribben JG. Poor concordance among nine immunohistochemistry classifiers of cell-of-origin for diffuse large B-cell lymphoma: implications for therapeutic strategies. *Clin Cancer Res*. 2013; 19:6686-6695.
  14. Choi WW, Weisenburger DD, Greiner TC, Piris MA, Banham AH, Delabie J, Braziel RM, Geng H, Iqbal J, Lenz G, Vose JM, Hans CP, Fu K, et al. A new immunostain algorithm classifies diffuse large B-cell lymphoma into molecular subtypes with high accuracy. *Clin Cancer Res*. 2009; 15:5494-5502.
  15. Hans CP, Weisenburger DD, Greiner TC, Gascoyne RD, Delabie J, Ott G, Muller-Hermelink HK, Campo E, Braziel RM, Jaffe ES, Pan Z, Farinha P, Smith LM, et al. Confirmation of the molecular classification of diffuse large B-cell lymphoma by immunohistochemistry using a tissue microarray. *Blood*. 2004; 103:275-282.
  16. Meyer PN, Fu K, Greiner TC, Smith LM, Delabie J, Gascoyne RD, Ott G, Rosenwald A, Braziel RM, Campo E, Vose JM, Lenz G, Staudt LM, et al. Immunohistochemical methods for predicting cell of origin and survival in patients with diffuse large B-cell lymphoma treated with rituximab. *J Clin Oncol*. 2011; 29:200-207.
  17. Barrans SL, Crouch S, Care MA, Worrillow L, Smith A, Patmore R, Westhead DR, Tooze R, Roman E, Jack AS. Whole genome expression profiling based on paraffin embedded tissue can be used to classify diffuse large B-cell lymphoma and predict clinical outcome. *Br J Haematol*. 2012; 159:441-453.
  18. Fu K, Weisenburger DD, Choi WW, Perry KD, Smith LM, Shi X, Hans CP, Greiner TC, Bierman PJ, Bociek RG, Armitage JO, Chan WC, Vose JM. Addition of rituximab to standard chemotherapy improves the survival of both the germinal center B-cell-like and non-germinal center B-cell-like subtypes of diffuse large B-cell lymphoma. *J Clin Oncol*. 2008; 26:4587-4594.
  19. Gleeson M, Hawkes EA, Cunningham D, Jack A, Linch D. Caution in the Use of Immunohistochemistry for Determination of Cell of Origin in Diffuse Large B-Cell Lymphoma. *J Clin Oncol*. 2015; 33:3215-3216.
  20. Gutierrez-Garcia G, Cardesa-Salzman T, Climent F, Gonzalez-Barca E, Mercadal S, Mate JL, Sancho JM, Arenillas L, Serrano S, Escoda L, Martinez S, Valera A, Martinez A, et al. Gene-expression profiling and not immunophenotypic algorithms predicts prognosis in patients with diffuse large B-cell lymphoma treated with immunochemotherapy. *Blood*. 2011; 117:4836-4843.
  21. Ott MM, Horn H, Kaufmann M, Ott G. The Hans classifier does not predict outcome in diffuse large B cell lymphoma in a large multicenter retrospective analysis of R-CHOP treated patients. *Leuk Res*. 2012; 36:544-545.
  22. Veldman-Jones MH, Brant R, Rooney C, Geh C, Emery H, Harbron CG, Wappett M, Sharpe A, Dymond M, Barrett JC, Harrington EA, Marshall G. Evaluating Robustness and Sensitivity of the NanoString Technologies nCounter Platform to Enable Multiplexed Gene Expression Analysis of Clinical Samples. *Cancer Res*. 2015; 75:2587-2593.
  23. Northcott PA, Shih DJ, Remke M, Cho YJ, Kool M, Hawkins C, Eberhart CG, Dubuc A, Guettouche T, Cardentey Y, Bouff  t E, Pomeroy SL, Marra M, et al. Rapid, reliable, and reproducible molecular sub-grouping of clinical medulloblastoma samples. *Acta Neuropathol*. 2012; 123:615-626.



24. Saba NF, Wilson M, Doho G, DaSilva J, Benjamin Isett R, Newman S, Chen ZG, Magliocca K, Rossi MR. Mutation and Transcriptional Profiling of Formalin-Fixed Paraffin Embedded Specimens as Companion Methods to Immunohistochemistry for Determining Therapeutic Targets in Oropharyngeal Squamous Cell Carcinoma (OPSCC): A Pilot of Proof of Principle. *Head Neck Pathol.* 2015; 9:223-235.
25. Scott DW, Chan FC, Hong F, Rogic S, Tan KL, Meissner B, Ben-Neriah S, Boyle M, Kridel R, Telenius A, Woolcock BW, Farinha P, Fisher RI, et al. Gene expression-based model using formalin-fixed paraffin-embedded biopsies predicts overall survival in advanced-stage classical Hodgkin lymphoma. *J Clin Oncol.* 2013; 31:692-700.
26. Norton N, Sun Z, Asmann YW, Serie DJ, Necela BM, Bhagwate A, Jen J, Eckloff BW, Kalari KR, Thompson KJ, Carr JM, Kachergus JM, Geiger XJ, et al. Gene expression, single nucleotide variant and fusion transcript discovery in archival material from breast tumors. *PLoS One.* 2013; 8:e81925.
27. Martin JW, Chilton-MacNeill S, Koti M, van Wijnen AJ, Squire JA, Zielenska M. Digital expression profiling identifies RUNX2, CDC5L, MDM2, RECQL4, and CDK4 as potential predictive biomarkers for neo-adjuvant chemotherapy response in paediatric osteosarcoma. *PLoS One.* 2014; 9:e95843.
28. Lee J, Sohn I, Do IG, Kim KM, Park SH, Park JO, Park YS, Lim HY, Sohn TS, Bae JM, Choi MG, Lim do H, Min BH, et al. Nanostring-based multigene assay to predict recurrence for gastric cancer patients after surgery. *PLoS One.* 2014; 9:e90133.
29. Sivendran S, Chang R, Pham L, Phelps RG, Harcharik ST, Hall LD, Bernardo SG, Moskalenko MM, Sivendran M, Fu Y, de Moll EH, Pan M, Moon JY, et al. Dissection of immune gene networks in primary melanoma tumors critical for antitumor surveillance of patients with stage II-III resectable disease. *J Invest Dermatol.* 2014; 134:2202-2211.
30. Stricker TP, Morales La Madrid A, Chlenski A, Guerrero L, Salwen HR, Gosiengfiao Y, Perlman EJ, Furman W, Bahrami A, Shohet JM, Zage PE, Hicks MJ, Shimada H, et al. Validation of a prognostic multi-gene signature in high-risk neuroblastoma using the high throughput digital NanoString nCounter system. *Mol Oncol.* 2014; 8:669-678.
31. Scott DW, Wright GW, Williams PM, Lih CJ, Walsh W, Jaffe ES, Rosenwald A, Campo E, Chan WC, Connors JM, Smeland EB, Mottok A, Braziel RM, et al. Determining cell-of-origin subtypes of diffuse large B-cell lymphoma using gene expression in formalin-fixed paraffin-embedded tissue. *Blood.* 2014; 123:1214-1217.
32. Reis PP, Waldron L, Goswami RS, Xu W, Xuan Y, Perez-Ordóñez B, Gullane P, Irish J, Jurisica I, Kamel-Reid S. mRNA transcript quantification in archival samples using multiplexed, color-coded probes. *BMC Biotechnol.* 2011; 11:46.
33. Wright G, Tan B, Rosenwald A, Hurt EH, Wiestner A, Staudt LM. A gene expression-based method to diagnose clinically distinct subgroups of diffuse large B cell lymphoma. *Proc Natl Acad Sci U S A.* 2003; 100:9991-9996.
34. Hill BT, Collie A, Radivoyevitch T, Hsi ED, Sweetenham J. Cell of origin determination in diffuse large b-cell lymphoma: Performance of immunohistochemical (IHC) algorithms and ability to predict outcome. *Blood.* 2011; 118:434 (abstr).
35. Scott DW, Mottok A, Ennishi D, Wright GW, Farinha P, Ben-Neriah S, Kridel R, Barry GS, Hother C, Abrisqueta P, Boyle M, Meissner B, Telenius A, et al. Prognostic Significance of Diffuse Large B-Cell Lymphoma Cell of Origin Determined by Digital Gene Expression in Formalin-Fixed Paraffin-Embedded Tissue Biopsies. *J Clin Oncol.* 2015; 33:2848-2856.
36. Beard RE, Abate-Daga D, Rosati SF, Zheng Z, Wunderlich JR, Rosenberg SA, Morgan RA. Gene expression profiling using nanostring digital RNA counting to identify potential target antigens for melanoma immunotherapy. *Clin Cancer Res.* 2013; 19:4941-4950.
37. Brumbaugh CD, Kim HJ, Giovacchini M, Pourmand N. NanoStriDE: normalization and differential expression analysis of NanoString nCounter data. *BMC Bioinformatics.* 2011; 12:479.
38. de Jong D, Rosenwald A, Chhanabhai M, Gaulard P, Klapper W, Lee A, Sander B, Thorns C, Campo E, Molina T, Norton A, Hagenbeek A, Horning S, et al. Immunohistochemical prognostic markers in diffuse large B-cell lymphoma: validation of tissue microarray as a prerequisite for broad clinical applications--a study from the Lunenburg Lymphoma Biomarker Consortium. *J Clin Oncol.* 2007; 25:805-812.
39. Jais JP, Haioun C, Molina TJ, Rickman DS, de Reynies A, Berger F, Gisselbrecht C, Briere J, Reyes F, Gaulard P, Feugier P, Labouyrie E, Tilly H, et al. The expression of 16 genes related to the cell of origin and immune response predicts survival in elderly patients with diffuse large B-cell lymphoma treated with CHOP and rituximab. *Leukemia.* 2008; 22:1917-1924.
40. Scott DW. Cell-of-Origin in Diffuse Large B-Cell Lymphoma: Are the Assays Ready for the Clinic? *Am Soc Clin Oncol Educ Book.* 2015:e458-466.